

Letters

Monitoring Molecular Adsorption on High-Area Titanium Dioxide via Modulated Diffraction of Visible Light

Xiaojun Dang, Keith J. Stevenson, and Joseph T. Hupp*

*Department of Chemistry and Institute for Environmental Catalysis, Northwestern University,
Evanston, Illinois 60208*

Received January 17, 2001

Patterned thin films of titanium dioxide (TiO_2), with micrometer-sized features, were prepared on transparent, conductive indium–tin oxide glass platforms via microtransfer molding and electrochemical deposition. The grating pattern produces optical diffraction, where the efficiency of diffraction (η) depends on the degree of contrast in refractive index between the patterned material and the surrounding medium. The refractive index of a representative micropatterned TiO_2 film (anatase) was estimated, via solvent index matching experiments, to be 2.72—a value sufficiently large to achieve good contrast with air or water. A new method, based on the measurement of changes in diffraction efficiency, is described for the detection and evaluation of organic chemical adsorption on various titanium dioxide surfaces. The strategy is illustrated for the vapor-phase adsorption of chloroform on high-area amorphous, anatase, and rutile forms of titanium dioxide. The uptake of 2,4,5-trichlorophenol from aqueous solutions by amorphous TiO_2 was also examined by the modulated optical-diffraction-grating technique.

Introduction

In addition to its widespread commercial use as a pigment, titanium dioxide is promising as both an electrode material (dye-sensitized photovoltaic materials,¹ thin-film batteries,² components of electrochromic devices,³ etc.) and as either a dispersed or immobilized catalyst for photo-degradation of aquatic and atmospheric pollutants.^{4,5} A particularly attractive feature of nanocrystalline forms of TiO_2 is their ability to form stable, high-area thin films, where the high area facilitates the adsorption of various molecular species. In dye sensitization experiments, the molecules adsorbed are chromophores and the objective is to collect large fractions of incident visible light using

a single monolayer of the chromophore. In photocatalytic experiments the adsorbates typically are pollutants. It is known, for example, that chlorinated micropollutants formed during municipal solid waste combustion,⁶ such as chlorinated alkanes, chlorinated benzenes, and chlorinated phenols, can be adsorbed on high-porosity titanium dioxide surfaces and subsequently photodegraded. One objective in photocatalyst design is to position the largest possible quantity of pollutant in direct contact with the catalytically active surface and, thereby, maximize pollutant degradation rates.

Given the significance of molecular adsorption for these applications, a need exists for methodologies capable of detecting adsorption. For chromophoric adsorbates, detection can be trivially accomplished via optical extinction measurements. For nonchromophoric or poorly chromophoric adsorbates, on the other hand, detection typically is less straightforward. One reasonably general method-

* To whom correspondence should be addressed. E-mail: jthupp@chem.nwu.edu.

(1) Hagfeld, A.; Grätzel, M. *Chem. Rev.* **1995**, *95*, 49.

(2) Ohzuku, T.; Takehara, Z.; Yoshizawa, S. *Electrochim. Acta* **1979**, *24*, 219.

(3) Ohzuku, T.; Hirai, T. *Electrochim. Acta* **1982**, *27*, 1263.

(4) Sopyan, L.; Murasawa, S.; Hashimoto, K.; Fujishima, A. *Chem. Lett.* **1994**, 723.

(5) Wold, A. *Chem. Mater.* **1993**, *5*, 280.

(6) Wikström, E.; Marklund, S. *Environ. Sci. Technol.* **2000**, *34*, 604.

ology, however, is quartz crystal microgravimetry (QCM).^{7,8} We describe here an alternative approach based on adsorbate-induced modulation of diffraction by micro-patterned surfaces. The approach is, in principle, similarly general with respect to adsorbate chemical composition, but potentially simpler and less expensive than the QCM approach. The specific systems examined here are vapor-phase adsorption of chloroform by amorphous, anatase, and rutile films and aqueous-phase adsorption of trichlorophenol by amorphous films. As shown below, the sensitivity of the diffraction method, in its present form, is about an order of magnitude poorer than that of very high quality QCM measurements.

Experimental Section

1. Preparation of Patterned TiO₂ Films. Patterned poly-(dimethylsiloxane) (PDMS) stamps for microtransfer molding were fabricated according to a previously described method.⁹ Briefly, PDMS stamps (with features of $5 \times 5 \mu\text{m}^2$ (lateral) with a depth of 180 nm) were "inked" with a thermally curable epoxy (TRA-CON F114) and were then placed on a clean conductive indium–tin oxide (ITO) platform. The ITO/epoxy/PDMS mold was cured at 60 °C for 1 h, and a patterned ITO platform was obtained.

Electrodeposition of TiO₂ on patterned ITO platforms was carried out in 50 mM TiCl₃ aqueous solution (pH 2.5).¹⁰ The epoxy-patterned ITO substrate acted as a working electrode. Suitable TiO₂ thin films were obtained after ~20 min by applying a fixed potential (0.04 V vs Ag/AgCl reference electrode). The resulting film was carefully washed with water, dried at room temperature, and finally annealed in air at 250, 450, or 650 °C for 1 h to yield, respectively, an amorphous, anatase or rutile-patterned TiO₂ film.¹¹

2. Diffraction Measurements. The light source was a He–Ne laser (633 nm emission) configured normal to the surface of the ITO-supported TiO₂ grating. The film was held in a sealed chamber (volume 46 mL) capped using an open-top closure with a nonabsorbing silicone/PTFE septum through which volatile organic chemical samples could be injected (for gas-phase experiments). Alternatively, for aqueous solution experiments, the grating was immersed in water in a quartz cell. The intensities of the undiffracted center beam (I_0) and one of the first-order diffraction beams (I_1) were monitored with photodiodes. The intensity of light passing through a transparent ITO substrate was taken as the total effective incident intensity (I_i). The diffraction efficiency, η , was defined and determined as follows:¹²

$$\eta = \frac{I_1 - I_0}{I_i} \quad (1)$$

Experimental data were collected using a personal computer via an in-house module written with Labview software (National Instruments Corp., Austin, TX).

3. Surface Characterization. Surface characterization was performed using a Digital Instruments Bioscope atomic force microscope. Images were obtained in tapping mode using etched silicon tips (125 μm cantilever length and resonance frequency 307–367 Hz, Digital Instruments). X-ray diffraction analysis was performed using a Rigaku Geigerflex X-ray diffractometer that employs a Cu K α line source. Data were obtained in a $\theta/2\theta$

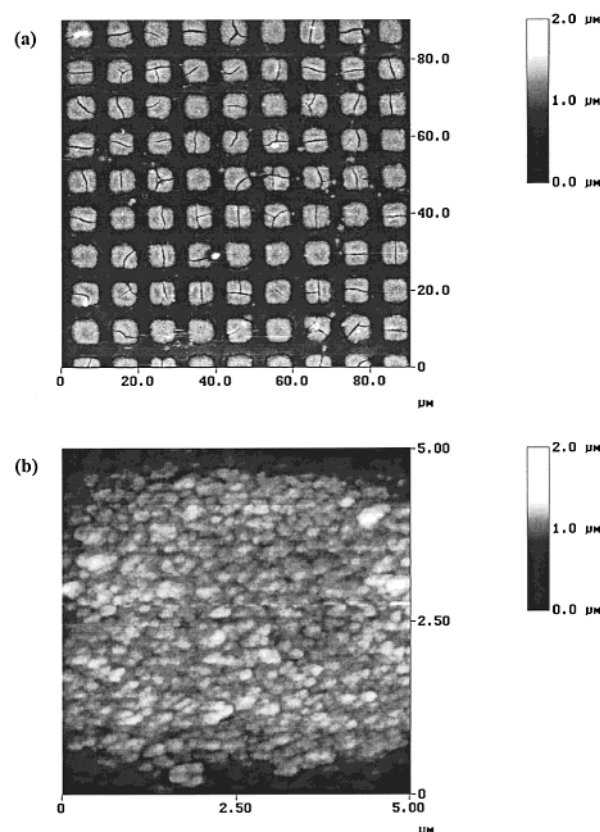


Figure 1. (a) A $90 \times 90 \mu\text{m}^2$ AFM height image of a patterned TiO₂ thin film on ITO prepared via microtransfer molding and electrochemical deposition methods. (b) A higher resolution AFM image ($5 \times 5 \mu\text{m}^2$ area) of a single-patterned square.

geometry and acquired between 20° and 60° every 0.2° (for anatase) or 0.1° (for the others) with integration time of 4 s.

Results and Discussion

1. Characterization of Patterned TiO₂/ITO Films.

Figure 1a shows a representative, large-scale atomic force microscopy (AFM) image of a patterned TiO₂ thin film prepared using a PDMS stamp made from a $5 \times 5 \mu\text{m}^2$ patterned lithographic master after annealing at 250 °C for 1 h. The regularity of this array was maintained over ~25 mm² (~33 000 squares). A higher resolution AFM image of a single patterned TiO₂ square is shown in Figure 1b, revealing the local surface topography, thickness (~465 nm), and roughness (~118 nm root-mean-square).

Both morphological and microstructural changes in TiO₂ can be induced by sintering processes.¹³ The existence of crystallinity and the identities of the crystalline structures of various films were determined via X-ray powder diffraction measurements (Figure 2). TiO₂ films heated at 250 °C displayed no net diffraction and are believed, therefore, to be amorphous. The diffraction pattern for films annealed at 450 °C shows anatase features, with an especially prominent (101) peak. The pattern for films sintered at 650 °C shows the (110) peak characteristic of rutile. Heat treatments are also known to be capable of substantially decreasing film thickness and surface roughness.¹⁴ These changes have been attributed to the

(7) Keefe, M. H.; Slone, R. V.; Hupp, J. T.; Czaplowski, K. F.; Snurr, R. Q.; Stern, C. L. *Langmuir* **2000**, *16*, 3964.

(8) Pinalli, R.; Nachtigall, F. F.; Ugozzoli, F.; Dalcanale, E. *Angew. Chem., Int. Ed.* **1999**, *38*, 2377.

(9) Stevenson, K. J.; Hurr, G. J.; Hupp, J. T. *Electrochem. Solid-State Lett.* **1998**, *2*, 175.

(10) Kavan, L.; O'Regan, B.; Kay, A.; Grätzel, M. *J. Electroanal. Chem.* **1993**, *346*, 291.

(11) Film thickness can be regulated by controlling the charge passed in the electrochemical deposition process. For instance, passing 0.45 C of charge produces, on average, films of ca. 500 nm.

(12) Nakajima, F.; Hirakawa, Y.; Kaneta, T.; Imasaka, T. *Anal. Chem.* **1999**, *71*, 2262.

(13) Anatase to rutile thermal transformation is dependent upon film preparation conditions, crystallite size, and amount of impurities. For instance, see: (a) Banfield, J. F.; Bischoff, B. L.; Anderson, M. A. *Chem. Geol.* **1993**, *110*, 211. (b) Cerrato, G.; Marchese, L.; Morterra, C. *Appl. Surf. Sci.* **1993**, *70*, 1993.

(14) Stevenson, K. J.; Hupp, J. T. *Electrochemical and Solid-State Lett.* **1999**, *2*, 497.

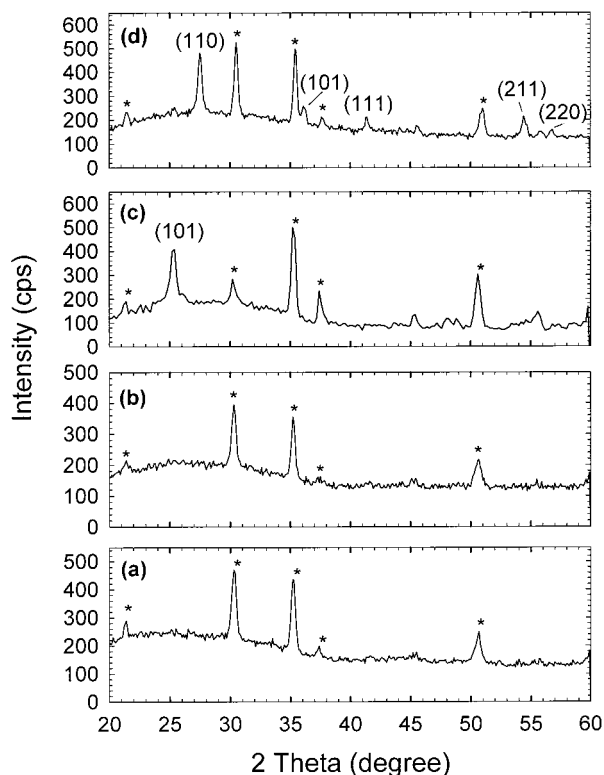


Figure 2. X-ray diffraction patterns for (a) blank ITO platform and TiO₂ films sintered at (b) 250 °C (amorphous), (c) 450 °C (anatase), and (d) 650 °C (rutile). Asterisk (*) denotes diffraction peaks of ITO.

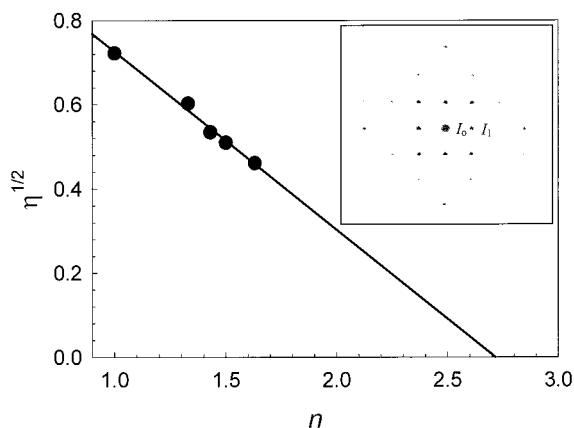


Figure 3. Square-root of diffraction efficiency ($\eta_{\text{norm}}^{1/2}$) versus refractive index (n) for a patterned anatase film in contact with air or with various solvents. The x -intercept of the best-fit straight line (i.e., complete index matching) corresponds to the refractive index of anatase. Inset: center portion of diffraction pattern for the grating in air.

loss of weakly coordinated water which results in film densification.

2. Estimation of Refractive Index of TiO₂. Passage of coherent, monochromatic, visible-region light through a patterned TiO₂ film yields an intense 2-D diffraction pattern (inset, Figure 3). Both TiO₂ and ITO are transparent at 633 nm; therefore diffraction arises solely from spatially periodic modulation of the real component of the film's refractive index. At a more quantitative level, the diffraction efficiency is expected to increase with increasing refractive index contrast between the patterned material and the surrounding medium, as shown ap-

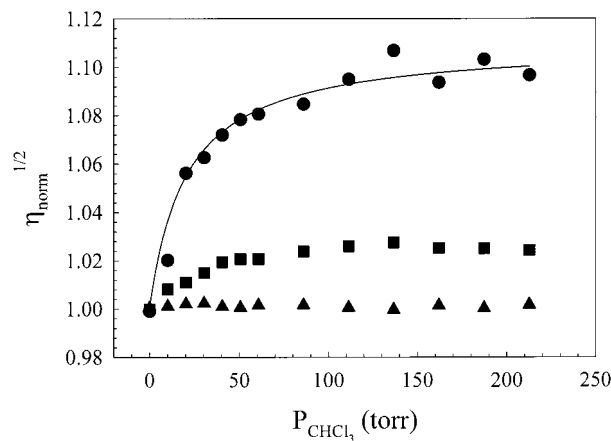


Figure 4. Vapor-phase adsorption isotherms for chloroform on amorphous (●), anatase (■) and rutile (▲) forms of TiO₂. η_{norm} is the diffraction efficiency normalized to 1 at a chloroform vapor pressure of zero. The solid line is a best fit of the amorphous TiO₂ data to a Langmuir isotherm.

proximately in eq 2¹⁵

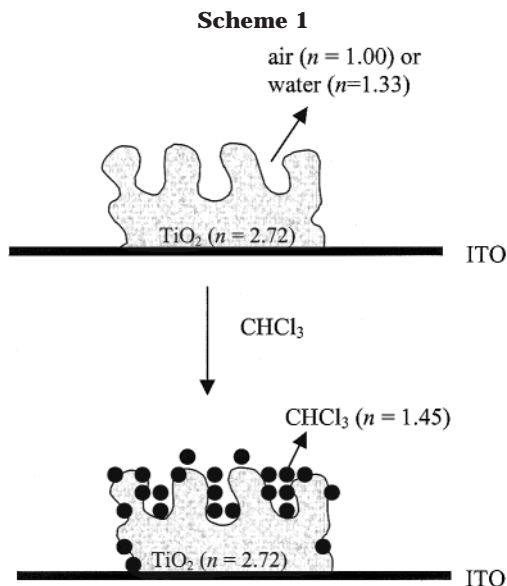
$$\eta = \left(\frac{\pi d \Delta n}{\lambda} \right)^2 \quad (2)$$

In the equation, d is the film thickness, Δn represents the degree of contrast in the refractive index, and λ is the wavelength of the incident light. Clearly, if the refractive index of the surrounding medium is changed, the refractive index contrast and, therefore, the diffraction efficiency will change. In the limit where the index of the medium has been changed sufficiently to achieve a value identical to the value for TiO₂, the diffraction efficiency will become zero. As shown in Figure 3, advantage can be taken of the medium dependence of η to determine the refractive index for the patterned TiO₂ material. In the figure, $\eta^{1/2}$ for a patterned anatase TiO₂ film has been recorded in air ($n = 1.00$) and in the presence of the following liquids: water ($n = 1.33$), cyclohexane ($n = 1.43$), benzene ($n = 1.50$), and carbon disulfide ($n = 1.63$). Extrapolation to $\eta^{1/2} = 0$ yields a n_{TiO_2} value of 2.72 at $\lambda = 633$ nm.

3. Molecular Adsorption. Although the results in the preceding section are ascribed to an index contrast between the medium and TiO₂, a slightly more sophisticated picture is one in which the index contrast is between the medium and a "composite" of the medium + high-porosity TiO₂ (Scheme 1). If the medium is air (essentially vacuum, $n = 1.00$), adsorption of any molecular species by the micropatterned TiO₂ will increase the index of refraction of the composite, since all molecules are characterized by n values greater than 1.00. Furthermore, the increase in $n_{\text{composite}}$ should be linear in the amount of molecular compound adsorbed. (For simplicity, we assume that the amount of compound adsorbing to the exposed low-surface-area ITO portion of the pattern is sufficiently small to be neglected.) Increases in $n_{\text{composite}}$ will increase the refractive index contrast, Δn , and therefore, increase the diffraction efficiency, η . From eq 2, changes in $\eta^{1/2}$ should report directly on changes in adsorbate surface concentration.

In Figure 4, a representative set of experiments involving chloroform adsorption by various micropatterned TiO₂ surfaces is shown. Increasing the partial pressure of CHCl₃ initially leads to increases in diffraction efficiency, followed by a plateauing of the diffraction response; i.e., Langmuir-type responses are observed. Normalized plots for the three

(15) Nelson, K. A.; Casalegno, R.; Miller, R. J. D.; Fayer, M. D. *J. Chem. Phys.* **1982**, *77*, 1144.



surfaces can be fit to a common isotherm with a common binding constant of ca. 0.05 Torr^{-1} . That the binding strength is similar for amorphous, anatase, and rutile forms of TiO₂ is not unreasonable given the probable nonspecific or van der Waals nature of the adsorption.

The striking differences in *amount* of chloroform adsorbed by the three surfaces were corroborated via QCM measurements (data not shown). We ascribe the differences to differences in surface area; thermal treatments are well-known to decrease the porosity and increase the density of nanocrystalline TiO₂ films.^{14,16} Assuming monolayer coverage by chloroform under limiting high vapor pressure conditions, QCM calibration of the amorphous film diffraction experiment in Figure 4 leads to an estimated effective surface area of 10 times the geometric area. On extension of the analyses to anatase and rutile, the effective surface areas are 3 and 0.3 times the geometric area, respectively. Note, however, that if adsorption also occurs on the ITO portions of the micropattern, the change in refractive index contrast upon adsorption to the TiO₂ portions will be smaller than otherwise expected, particularly for the lowest area film, thereby falsely depressing the estimated area for low area films. Returning to the QCM calibration of the amorphous film, we find, based on an estimated differential measurement limit of 0.5% of the normalized diffraction efficiency, a detection limit of $\sim 2 \text{ ng}$ of adsorbed CHCl₃ ($\sim 20 \text{ pmol}$) per square millimeter of grating or $\sim 0.5 \text{ ng}$ ($\sim 4 \text{ pmol}$) per square millimeter of TiO₂ (geometric area). This is roughly an order of magnitude poorer than that achievable in very high quality QCM experiments. We believe, however, that the signal-to-noise ratio, and therefore the detection limit, of the grating measurement can be significantly improved.

Finally, we find that diffraction-based adsorption measurements can also be made in aqueous solution environments, in this case with 2,4,5-trichlorophenol (TCP) as the adsorbate. As shown in Figure 5, TCP adsorption on a micropatterned amorphous TiO₂ film, in

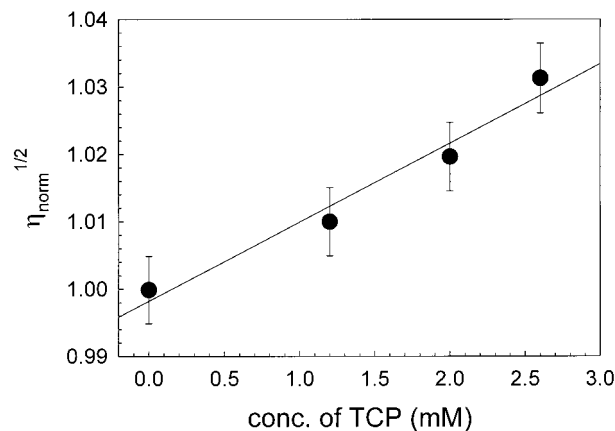


Figure 5. Plot of $\eta_{\text{norm}}^{1/2}$ vs concentration of 2,4,5-trichlorophenol in aqueous solution. The grating film used was amorphous TiO₂.

contact with water, induces changes in diffraction efficiency—where adsorption again has been corroborated via QCM. Since the refractive index of water is higher than that of air, the refractive index contrast of the patterned material and the surrounding medium is weaker in aqueous environments. Therefore, the sensitivity of the aqueous diffraction experiment is expected to be about 3-fold less than that of vapor phase experiments. To elaborate briefly, the pertinent refractive-index-contrast comparisons are (1) air vs an air/TiO₂ composite (patterned region), and air vs an air ($n = 1.00$)/adsorbed trichlorophenol ($n \approx 1.5$)/TiO₂ ($n = 2.72$) composite (see Scheme 1), and (2) water vs a water/TiO₂ composite, and water vs a water ($n = 1.33$)/adsorbed trichlorophenol/TiO₂ composite. The refractive index contrast between the medium and the medium/TiO₂ composite determines the overall diffraction efficiency. The degree of contrast between the medium and the adsorbate, however, determines the degree of *change* in contrast and, therefore, the sensitivity of the measurement of adsorption.

Conclusions

Adsorption-induced modulation of refractive index contrast by micropatterned TiO₂ films in contact with air or water can be used to detect and quantify molecular adsorption. Because all molecules possess refractive indices greater than air (essentially vacuum) and most have indices greater than water, the diffraction methodology should prove applicable to almost all adsorbates. As such, it offers a potential advantage over methods that rely upon adsorbate-specific absorption, luminescence, or redox responses. In its present form, the detection limit is roughly 0.5 ng of adsorbed material per square millimeter of TiO₂ film (geometric area). A more detailed account of the influence of film microstructure (e.g., porosity and crystallinity) on molecular adsorption will be presented elsewhere.

Acknowledgment. We gratefully acknowledge Dr. Gary Mines and Aaron Massari for their assistance with the experimental setup and for helpful discussion. We thank the Office of Naval Research and the Northwestern University Institute for Environmental Catalysis for financial support.

LA010096Q

(16) Similar to our observation of WO₃, preliminary studies indicate that sintering TiO₂ films at higher temperatures (450°C for 1 h) results in $\sim 8\%$ decrease in film thickness and $\sim 10\%$ decrease in root mean square surface roughness.